Macromolecules

Article

pubs.acs.org/Macromolecules

Dynamics and Large Strain Behavior of Self-Healing Hydrogels with and without Surfactants

Deniz C. Tuncaboylu,[†] Melahat Sahin,[†] Aslihan Argun,[†] Wilhelm Oppermann,*[,‡] and Oguz Okay*[,†]

[†]Department of Chemistry, Istanbul Technical University, 34469 Maslak, Istanbul, Turkey

[‡]Institute of Physical Chemistry, Clausthal University of Technology, 38678 Clausthal-Zellerfeld, Germany

Supporting Information

ABSTRACT: Polyacrylamide hydrogels formed via hydrophobic interactions between stearyl groups in aqueous micellar solution of sodium dodecyl sulfate (SDS) present two faces depending on which state they are. The gels containing SDS micelles exhibit, in addition to the fast mode, a slow relaxation mode in dynamic light scattering (DLS) and time-dependent elastic moduli, indicating the temporary nature of the hydrophobic associations having lifetimes of the order of seconds to milliseconds. The gels where SDS had been removed after their preparation behave similar to chemically cross-linked ones with time-independent elastic moduli, a high degree of spatial inhomogeneity, and a single relaxation mode in DLS. Because of this drastic structural change, the physical gels are insoluble in water with a gel fraction close to unity. In surfactant containing gels, a large proportion of physical cross-links dissociate under force, but they do so reversibly, if the force is removed they reform again. The reversible disengagements of the hydrophobic units building the physical cross-links leads to a self-healing efficiency of nearly 100%, while no such healing behavior was observed after extraction of SDS due to the loss of the reversible nature of the cross-linkages.

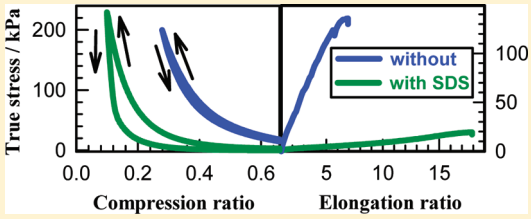

INTRODUCTION

Aqueous solutions of hydrophobically modified hydrophilic polymers constitute a class of soft materials with remarkable rheological properties.[1,2] Above a certain polymer concentration, the hydrophobic groups in such associative polymers are involved in intermolecular associations that act as reversible breakable cross-links creating a transient 3D polymer network. A simple method to obtain associative polymers is the free radical micellar polymerization technique, as first described by Candau and co-workers.[1−8] In this technique, a water-insoluble hydrophobic monomer solubilized within the micelles is copolymerized with a hydrophilic monomer such as acrylamide (AAm) in aqueous solutions by free-radical addition polymerization. Because of high local concentration of the hydrophobe within the micelles, the hydrophobic monomers are distributed as random blocks along the hydrophilic polymer backbone. One limitation of this technique is that large hydrophobes such as stearyl methacrylate (C18) or dococyl acrylate (C22) cannot be solubilized within the micelles due to the very low water solubility of these monomers.[9−12] Incorporation of blocks of large hydrophobes into a hydrophilic polymer backbone would produce strong and long-lived hydrophobic associations.

We have recently shown that large hydrophobes can be solubilized in a micellar solution of sodium dodecyl sulfate (SDS) provided that an electrolyte, such as NaCl, has been added in sufficient amount.[9] Salt leads to micellar growth[13,14] and, hence, solubilization of the hydrophobes within the grown SDS micelles. As illustrated in Figure 1, after solubilization of the large hydrophobes C18 or C22 within the wormlike SDS micelles of salt solutions, they could be copolymerized with AAm to obtain physical hydrogels. The surfactant-containing gels formed using C18 blocks as physical cross-links exhibit unique characteristics such as insolubility in water but solubility in SDS solutions, nonergodicity, self-healing, and a high degree of toughness.[9]

However, when SDS micelles are removed from the physical gels, they become fragile and do not exhibit the initial mechanical performances. Understanding what gives these surfactant-containing gels toughness and self-healing ability could be essential for the design of future self-healing soft materials and this was the aim of this study. Moreover, although the physical gels we reported before were in a state close to the critical gel state with a power-law frequency dependence in their viscoelastic moduli, they were insoluble in water with a gel fraction close to unity.[9] It was also of fundamental interest to explain the apparent contradiction that a critical gel could remain stable in water.

Here, we prepared physical gels by micellar copolymerization of AAm with 2 mol % C18 in aqueous SDS−NaCl solutions. The initial monomer concentration was varied over a wide range. By increasing the polymer concentration at the gel preparation, we were able to obtain strong gels enabling determination of their large strain behavior. We present and characterize in this paper two series of physical gels: one series still containing SDS micelles and another one where the SDS micelles had been removed after preparation. Dynamic

Received: December 9, 2011
Revised: January 24, 2012
Published: February 6, 2012

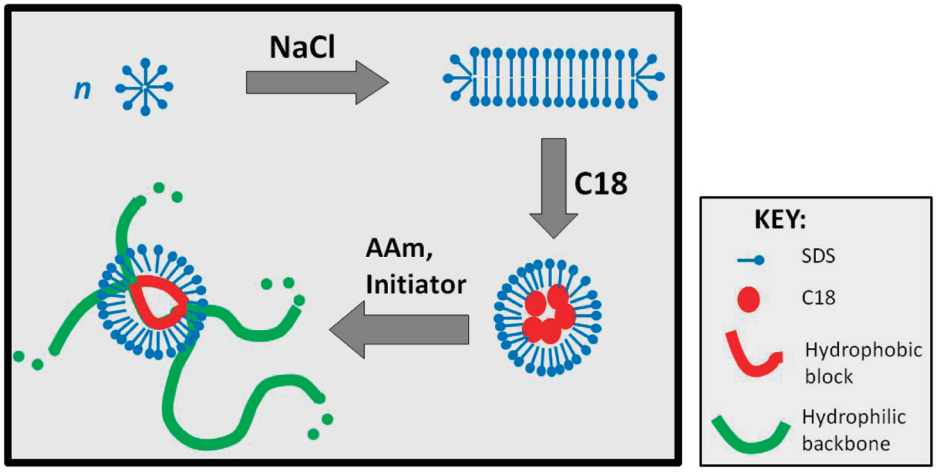

Figure 1. Cartoon showing the formation of surfactant containing physical gels in aqueous SDS−NaCl solutions via hydrophobic C18 blocks.

properties of the gels were investigated by dynamic light scattering (DLS) and rheometry, while their large-strain mechanical and self-healing performances were determined by uniaxial elongation or compression tests. We will show that the physical gels without SDS micelles behave similar to chemically cross-linked gels: they exhibit time-independent dynamic moduli and a single relaxation mode in DLS. When micelles are present, the hydrophobic interactions are weakened, thereby increasing the viscoelastic dissipation in the gel sample. This is the key factor for self-healing. After fracture, strong hydrophobic interactions localized across the damage surfaces together with the internal dynamics of surfactant containing gels leads to the renewal of hydrophobic associations and self-healing at room temperature.

EXPERIMENTAL PART

Materials. Acrylamide (AAm, Merck), sodium dodecyl sulfate (SDS, Sigma), ammonium persulfate (APS, Merck), *N,N,N′,N′*-tetramethylethylenediamine (TEMED, Merck), and NaCl (Merck) were used as received. Commercially available stearyl methacrylate (C18, Fluka) consists of 65% *n*-octadecyl methacrylate and 35% *n*-hexadecyl methacrylate. Micellar copolymerization of AAm with C18 was conducted at 25 °C for 24 h in the presence of an APS (3.5 mM)−TEMED (0.25% v/v) redox initiator system. SDS and NaCl concentrations were set to 7% w/v (0.24 M) and 0.5 M, respectively. C18 content of the monomer mixture was also fixed at 2 mol % while the total monomer concentration was varied between 5% and 15% w/v. The gel preparation procedure was the same as in our previous study.[9] For the swelling and mechanical measurements, the copolymerization reactions were carried out in plastic syringes of 4 mm internal diameters. For the dynamic light scattering measurements, the reactions were conducted in light scattering vials after filtration of the gelation solutions through Nylon membrane filters with a pore size of 0.2 μm.

Quantification of the Solubilization of C18 in SDS−NaCl Solutions. The amount of C18 solubilized in the micelles was estimated by measuring the transmittance of SDS−NaCl solutions containing various amounts of C18 on a T80 UV−vis spectrophotometer. The transmittance at 500 nm was plotted as a function of the added amount of C18 in the SDS−NaCl solution, and the solubilization extent of C18 was determined by the curve break (Figure S1).

Rheological Experiments. Gelation reactions were carried out at 25 °C within the rheometer (Gemini 150 rheometer system, Bohlin Instruments) equipped with a cone-and-plate geometry with a cone angle of 4° and diameter of 40 mm. The instrument was equipped with a Peltier device for temperature control. The reactions were monitored at an angular frequency ω of 6.3 rad/s and a deformation amplitude γ_0 = 0.01. After a reaction time of 3 h, the dynamic moduli of the reaction solutions approached limiting values (Figure S2). Then, frequency-sweep tests and stress-relaxation experiments were carried out at 25 °C, as described before.[9]

Dynamic Light Scattering (DLS) Measurements. DLS measurements were performed at 25 °C using ALV/CGS-3 compact goniometer (ALV, Langen, Germany) equipped with a cuvette rotation/translation unit (CRTU) and a He−Ne laser (22 mW, λ = 632.8 nm). The scattering angle θ was varied between 50° and 130°. Details about the instrument were described before.[9] The time-average intensity correlation functions $g_T^{(2)}(q\ \tau)$ of gels were acquired at 100 different sample positions selected by randomly moving the CRTU before each run. The acquisition time for each run was 30 s. The short-time limit of $g_T^{(2)}(q,\tau)$ can be related to an apparent diffusion coefficient, D_A, via[15,16]

$$D_A = -\frac{1}{2q^2}\lim_{\tau\to 0}\frac{d(\ln(g_T^{(2)}(q,\tau)-1))}{d\tau} \quad (1)$$

where q is the scattering vector, $q = (4\pi n/\lambda)\sin(\theta/2)$, n is the refractive index of the solvent, τ is the decay time, and subscript T denotes time average. For nonergodic media like polymer gels, D_A and, likewise, the time-averaged scattering intensity $\langle I(q)\rangle_T$ vary randomly with sample position. $\langle I(q)\rangle_T$ has two contributions: one from static inhomogeneities (frozen structure) and the other from dynamic fluctuations according to the following equation:[15−17]

$$\langle I(q)\rangle_T = I_C(q) + \langle I_F(q)\rangle_T \quad (2)$$

where $I_C(q)$ and $\langle I_F(q)\rangle_T$ are the scattered intensities due to the frozen structure and liquidlike concentration fluctuations, respectively. To separate $\langle I(q)\rangle_T$ into its two parts, we follow the method proposed by Joosten et al.[15] Treating the system by the partial heterodyne approach, one obtains

$$\frac{\langle I(q)\rangle_T}{D_A} = \frac{2\langle I(q)\rangle_T}{D} - \frac{\langle I_F(q)\rangle_T}{D} \quad (3)$$

The cooperative diffusion coefficient D and the fluctuating component of the scattering intensity $\langle I_F(q)\rangle_T$ of the present hydrogels were obtained by plotting $\langle I(q)\rangle_T/D_A$ vs $\langle I(q)\rangle_T$ data recorded at 100 different sample positions (Figure S3). The dynamic correlation length ξ was evaluated by $\xi = kT/(6\pi\eta D)$, where η is the viscosity of the medium (0.89 mPa·s) and kT is the Boltzmann energy.

For ergodic media like surfactant solutions, the scattered intensity contains only a fluctuating component and independent of sample position. $g_T^{(2)}(q,\tau)$ is then equivalent to an ensemble-averaged intensity correlation function and can be written as the Laplace

dx.doi.org/10.1021/ma202672y | Macromolecules 2012, 45, 1991−2000

transform of the distribution of relaxation rates, $G(\Gamma)$ (we disregard a coherence factor):

$$g_T^{(2)}(q, \tau) - 1 = [\int_0^\infty G(\Gamma) \exp(-\Gamma\tau)\, d\Gamma]^2 \quad (4)$$

where Γ is the characteristic relaxation rate. $G(\Gamma)$ values at five angles (50°, 70°, 90°, 110°, and 130°) were evaluated with an inverse Laplace transform of $g_T^{(2)}(q,\tau) - 1$ with the integrated ALV software (Figure S4). Relaxation rates of the fast (Γ_{fast}) and slow modes (Γ_{slow}) were obtained from the peak values of Γ in $G(\Gamma)$s. For a diffusion process, the relaxation rate of a particular mode is q^2 dependent and is related to the diffusion coefficient as $\Gamma = Dq^2$.

Gel Fractions and Swelling Measurements. Cylindrical hydrogel samples (diameter 4 mm, length about 6 cm) were immersed in a large excess of water at 24 °C for at least 15 days by replacing water every day to extract any soluble species. The masses m of the gel samples were monitored as a function of swelling time by weighing the samples. Relative weight swelling ratio m_{rel} of gels was calculated as $m_{rel} = m/m_0$, where m_0 is the initial mass of the gel sample. Then, the equilibrium swollen gel samples with relative masses $m_{rel,eq}$ were taken out of water and immersed in liquid nitrogen for 5 min before they were freeze-dried. The amount of SDS released from the gels during their swelling was estimated using the methylene blue (MB) method.[18] For this purpose, swelling tests were carried out as described above, except that the volume of external solution was fixed at 100 mL. Solution samples were taken at various time intervals, just before replacing water, and subjected to MB method. The amount of SDS released was calculated as $10^2 m_{SDS,t}/(m_0 C_{SDS})$, where $m_{SDS,t}$ is the mass of SDS in the external solution at time t and C_{SDS} is the initial SDS concentration of gel samples (0.07 g/mL). The cumulative release of SDS was obtained by summing up SDS released % data over all times. To check for completeness of SDS extraction from gels, dry samples were inspected by energy dispersive X-ray spectroscopy (EDS) performed on a scanning electron microscope (Jeol 6335F) using Oxford-INCA/ISIS software. EDS spectra were acquired and used for X-ray mapping of sulfur (detection limit: 0.1%) and other elements present in the samples.

The gel fraction W_g, that is, the conversion of monomers to the water-insoluble polymer (mass of cross-linked polymer/initial mass of the monomer), was calculated from the masses of dry, extracted polymer network and from the comonomer feed. The volume fractions of physically cross-linked PAAm after the gel preparation and in the equilibrium swollen gel, ν_2^0 and ν_2, respectively, were calculated as

$$\nu_2^0 = 10^{-2}\rho^{-1}C_0 W_g \quad (5a)$$

$$\nu_2 = \left[1 + \left(\frac{m_{rel,eq}}{\nu_2^0} - \rho\right)\right]^{-1} \quad (5b)$$

where ρ is the density of PAAm (1.35 g/mL).[19] The linear swelling ratio α of the gels with respect to the state of preparation was calculated from the polymer volume fractions as $\alpha = (\nu_2^0/\nu_2)^{1/3}$.

Uniaxial Compression Measurements. The measurements were performed in a thermostated room at 24 ± 0.5 °C on gel samples both in the state of preparation and after equilibrium swelling in water. Cyclic compression experiments were performed on a Zwick Roell test machine using a 10 N load cell. The cylindrical hydrogel sample of about 4 mm diameter and 6 mm length was placed between the plates of the instrument. Before the test, an initial compressive contact to 0.004 ± 0.003 N was applied to ensure a complete contact between the gel and the plates. Cyclic tests were conducted with a compression step performed at a constant crosshead speed of 5 mm/min to a maximum load (varied between 0.5 and 4 N), followed by immediate retraction to zero displacement and a waiting time of 2 min, until the next cycle of compression. Load and displacement data were collected during the experiment. Compressive stress was presented by its nominal σ_{nom} or true values σ_{true} (= $\lambda\sigma_{nom}$), which are the forces per cross-sectional area of the undeformed and deformed gel specimen, respectively, while the strain is given by λ, the deformation ratio (deformed length/initial length). The stress–strain isotherms at low compression ratios were measured by using an apparatus previously described by our group.[20] Briefly, cylindrical gel sample (diameter 4 mm, length 7 mm) was placed on a digital balance (Sartorius BP221S). A load was transmitted vertically to the gel through a rod fitted with a PTFE end-plate. The force acting on the gel was calculated from the reading of the balance while the resulting deformation was measured using a digital comparator (IDC type Digimatic Indicator 543-262, Mitutoyo Co.), which was sensitive to displacements of 10^{-3} mm. The force and the resulting deformation were recorded after 10 s of relaxation. The measurements were conducted up to about 20% compression with increments of ca. 1%. The modulus G_t of gels after a relaxation time t = 10 s was determined from the slope of the linear dependence

$$\sigma_{nom} = -G_t(\lambda - \lambda^{-2}) \quad (6)$$

Typical stress–strain data plotted according to eq 6 are shown in Figure S5 for the hydrogels before and after swelling in water.

Uniaxial Elongation Measurements. The measurements were performed on cylindrical hydrogel samples of about 4 mm in diameter on a Zwick Roell test machine using a 500 N load cell under the following conditions: crosshead speed = 50 mm/min, sample length between jaws = 13 ± 3 mm. The tensile strength and percentage elongation at break were recorded. For reproducibility, at least six samples were measured for each gel, and the results were averaged.

RESULTS AND DISCUSSION

Preparation of Physical Gels with and without Surfactant. Physical gels were prepared by the micellar copolymerization of AAm with C18 in aqueous SDS–NaCl solutions. C18 content of the monomer mixture (C18 + AAm) was fixed at 2 mol % while the initial monomer concentration C_0 was varied between 5% and 15%. The presence of NaCl in the reaction solution induced the micellar growth (see the next section) and, hence, solubilization of the hydrophobe C18 within the SDS micelles. The maximum solubility of C18 in the reaction solution was determined as 1.2% w/v, corresponding to C_0 = 15% (Figure S1). Indeed, transparent gels were obtained in the range of C_0 between 5% and 15% while at larger concentrations translucent gels were obtained. We therefore limited our investigation to gels formed at or below C_0 = 15%.

To obtain physical gels free of SDS micelles, the gel samples were extracted in water at 24 °C. Figure 2 shows the data

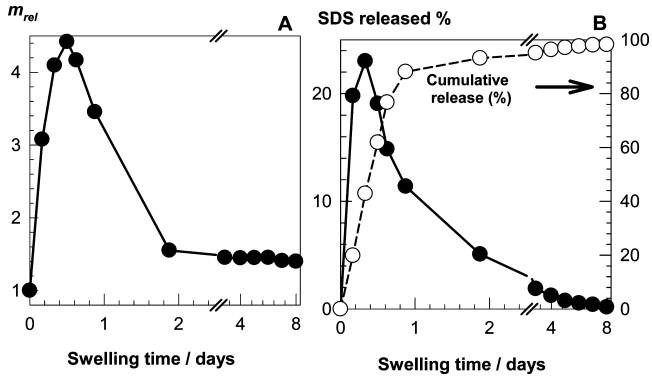

Figure 2. Relative weight swelling ratio m_{rel} of the physical gel (A) and the amount of SDS released from the gel (B) plotted against the swelling time in water. C_0 = 10%.

obtained during the extraction of a gel sample formed at C_0 = 10%, where the relative gel mass m_{rel} and the released amount of SDS from the gel (in %) are plotted as a function of the

dx.doi.org/10.1021/ma202672y | Macromolecules 2012, 45, 1991–2000

swelling time. At short swelling times, the gel exhibits a large swelling ratio due to the osmotic pressure of SDS counterions inside the gel network. As SDS is progressively extracted from the network, the osmotic effect disappears and the gel gradually converts into a nonionic gel having a markedly reduced swelling ratio ($m_{rel,eq}$ = 1.3 ± 0.2 for C_0 = 5−15%). Cumulative SDS release data in Figure 2B reveal that, after a swelling time of about 8 days, all SDS was extracted from the gels. Indeed, sulfur analyses of freeze-dried gel samples formed between C_0 = 5% and 15% gave no sulfur (<0.1%), indicating complete SDS extraction.

The characteristics of the physical gels before and after swelling in water are collected in Table 1. The average gel fraction W_g is 0.86 ± 0.02, demonstrating strong hydrophobic associations between the PAAm chains which could not be destroyed during the expansion of the gels in water. The polymer concentration ν_2 of the gels swollen to equilibrium is a little lower than the value ν_2^0 at the state of gel preparation. The linear swelling ratio α increases slightly with rising C_0 from 1.04 to 1.16, suggesting that the network chains are in the Gaussian regime.[20,21] Also, the fact that the equilibrium swelling ratio is considerably lower than the maximum swelling (cf. Figure 2A) is a strong indication that the network chains are in the Gaussian regime. In contrast, we observed that the gels which are soft at the state of preparation become stiff upon swelling in water. To quantify this behavior, we measured the elastic modulus G_t of cylindrical gel samples (diameter 4 mm, length 7 mm) after a relaxation time t of 10 s. Table 1 also contains the moduli data of gels before and after swelling in water. The equilibrium swollen gels exhibit 3−8-fold larger elastic moduli than those in the preparation state. As the degrees of dilution of the network chains before and after swelling are close together (Table 1), this increase reveals the occurrence of structural transformations during the removal of the surfactant micelles from the gel network.

Table 1. Properties of the Physical Gels with and without SDS

		after preparation state		after equilibrium swelling in water		
C_0 (% w/v)	W_g	G_t (kPa)	ν_2^0	G_t (kPa)	ν_2	α
5	0.83	*a*	0.031	*a*	0.027	1.04
6	0.87	0.14	0.039	*a*	0.032	1.06
7	0.86	0.34	0.045	2.0	0.037	1.06
8	0.88	0.64	0.052	4.8	0.042	1.07
9	0.86	1.0	0.057	6.8	0.045	1.08
10	0.87	1.5	0.064	8.1	0.049	1.09
15	0.83	4.9	0.092	13.0	0.058	1.16

[a]Gels were too weak to withstand the elasticity measurements.

Dynamics of Gelation Solutions and Physical Gels. DLS measurements were conducted at various preparation steps of the gelation solutions, i.e., before and after additions of NaCl, C18, or AAm into the SDS solution as well as after polymerization and after removal of SDS micelles. The time-average intensity correlation functions (ICFs) of the solutions and gels were recorded at five angles (θ) between 50° and 130°. Figures 3A and 3B show typical ICFs obtained at θ = 90° from solutions and gels, respectively. ICF of the SDS−water solution exhibits both fast and slow relaxation modes. This is similar to

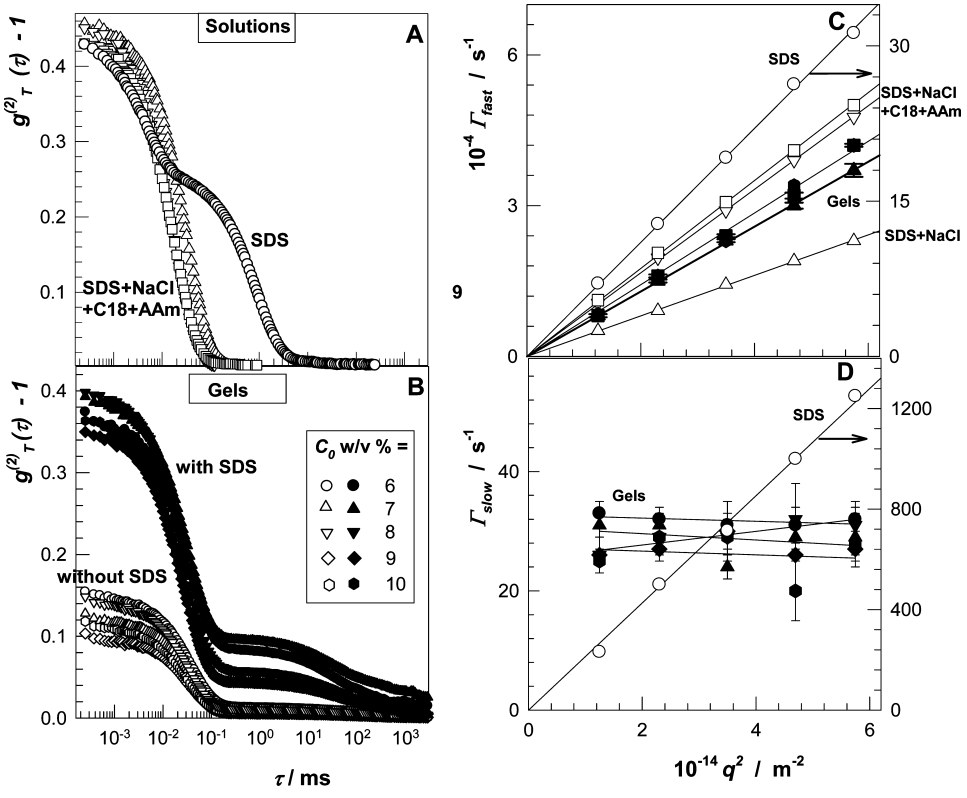

Figure 3. (A, B) ICFs of SDS solutions (A) and physical gels (B). θ = 90°. SDS solutions without (○) and with NaCl (△), NaCl + C18 (▽), and NaCl + C18 + AAm (□). The amounts of C18 and AAm correspond to the preparation recipe of 10% gel. However, amounts corresponding to 5−10% gels do not affect the results. Filled and open symbols in (B) represent data for gels with and without SDS, respectively. (C, D) Relaxation rates of the fast (Γ_{fast}) and slow modes (Γ_{slow}) plotted against q^2 for gels and solutions. The symbols are the same as in (A) and (B).

dx.doi.org/10.1021/ma202672y | Macromolecules 2012, 45, 1991−2000

polyelectrolyte solutions where a fast and a slow mode occur in salt-free conditions. These relaxations merge into one upon addition of salt.[22] Likewise, the addition of NaCl (0.5 M) and of monomers into the SDS solution results in the disappearance of the slow mode. After formation of the physical gels, a slow mode appears again on an even longer time scale (Figure 3B). However, when the SDS micelles are removed from the gels, the slow mode disappears.

Additional information can be obtained from the scattering vector dependencies of the relaxation rates. The relaxation rates of the fast (Γ_{fast}) and slow modes (Γ_{slow}) were obtained from the peak positions in the relaxation rate distribution functions $G(\Gamma)$, some examples of which are given in Figure S4. In Figures 3C and 3D, Γ_{fast} and Γ_{slow} are plotted against q^2, respectively. For SDS−water solution, Γ_{fast} and Γ_{slow} are both proportional to q^2, demonstrating diffusive processes. The hydrodynamic correlation length ξ on the basis of the fast mode was calculated as 0.5 nm for SDS micelles in water, while after addition of NaCl, it increases to 6.1 nm due to the formation of wormlike micelles.[9,23−25] Addition of C18 and AAm into the SDS−NaCl solution decreases again the correlation length to 3 nm due to the oil-induced structural change of wormlike micelles.[9,26−30] In contrast to the slow relaxation mode of the SDS solution, the slow mode of gels containing SDS (~30 ms) is independent of the scattering vector q (filled symbols in Figure 3D), demonstrating that it does not represent a diffusive process but is related to the structural relaxation of the physical network. Thus, the ICFs indicate a structural relaxation in physical gels on the time scales of milliseconds. This process only occurs in the presence of SDS micelles, it seems to disappear when the SDS is removed.

Rheological measurements are another means of studying the dynamic properties of the gels. Figures 4A and 4B show the frequency dependencies of the elastic modulus G' (filled symbols), viscous modulus G'' (open symbols), and tan δ (= G''/G', lines) for the gels (C_0 = 10%) with (A) or without SDS (B). In Figures 4C and 4D, the relaxation moduli $G(t)$ of the same gels, obtained from stress relaxation measurements, are plotted against time t at different strains γ_0. The gel containing SDS exhibits time-dependent dynamic moduli with a plateau modulus at high frequencies (10^2 rad/s) and a loss factor above 0.1 indicating the temporary nature of the hydrophobic associations having lifetimes of the order of seconds to milliseconds. After extraction of SDS, the dynamic moduli become nearly time independent and the loss factor decreases below 0.1 corresponding solidlike behavior. Similar results were also obtained for other gel samples formed at various concentrations (Figure S6).

On the basis of these measurements, we conclude that, when SDS micelles are present, the cross-links are reversible due to the local solubilization of the hydrophobic associations so that the gels are weak. After extraction of SDS, direct exposure of the hydrophobic associations to the aqueous environment increases their lifetimes so that the gels behave mostly like being covalently cross-linked ones with time-independent dynamic moduli and a single mode relaxation in DLS. The results also demonstrate that the presence of surfactant micelles is responsible for the slow mode of the physical gels. Previous studies show a slow relaxation in the micellar kinetics on the time scale of milliseconds to seconds, corresponding to the dissolution of a micelle into individual surfactant molecules.[31] Since the breakup of a micelle around the hydrophobic blocks

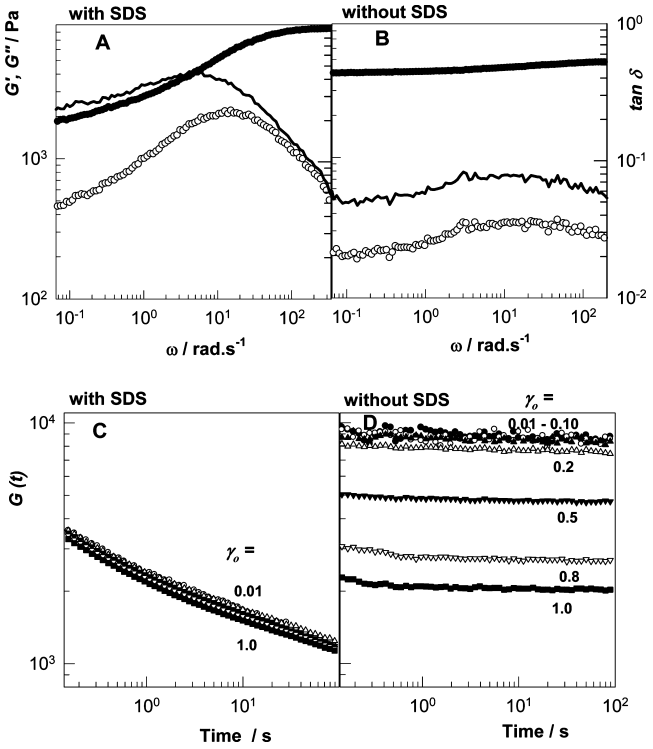

Figure 4. (A, B) G' (filled symbols), G'' (open symbols), and tan δ (lines) of gels with (A) and without SDS (B) shown as a function of angular frequency ω. C_0 = 10%; γ_0 = 0.01. (C, D) Relaxation modulus $G(t)$ as a function of time t for various strains γ_0 for gels with (C) and without SDS (D). C_0 = 10%; γ_0 = 0.01 (●), 0.05 (○), 0.10 (▲), 0.20 (△), 0.50 (▼), 0.80 (▽), and 1.0 s (■).

will enhance the hydrophobic interactions at this location, while its re-formation will decrease these interactions again, it is likely that the micellar kinetics and resulting temporary strong associations are responsible for the slow network relaxations in SDS containing physical gels.

Additionally, we point out that the water insolubility of the present physical gels, even those in a critical gel state,[9] is in accord with the above findings. During the swelling process, the removal of SDS from the gels increases the lifetime of the associations so that the gels become increasingly stable as SDS is progressively extracted. Conversely, if swelling is performed without extraction of SDS (this requires an excess of SDS in the swelling medium), the gels should dissolve due to the weak hydrophobic associations. This was indeed observed. In Figure 5, the relative mass m_{rel} of gel samples formed at C_0 = 10% is shown as a function of the swelling time in SDS−water solutions. At or above 5% SDS concentrations, the gels completely dissolve within 1−3 weeks while they remain stable at lower SDS concentrations. Because of the weakening of the hydrophobic associations with increasing surfactant concentration, the higher the SDS concentration in the external solution, the shorter the time period required for the gel-to-sol transition and the lower is the gel mass at this transition.

Structural Inhomogeneity of Gels with and without SDS. Figure 3B shows that the initial amplitude of the ICF significantly decreases after extraction of SDS micelles, indicating increasing extent of frozen concentration fluctuations. To account for the nonergodicity of gels, the time-averaged scattering intensity $\langle I \rangle_T$ at θ = 90° was recorded at a hundred different sample positions. Figure 6A shows the

dx.doi.org/10.1021/ma202672y | Macromolecules 2012, 45, 1991−2000

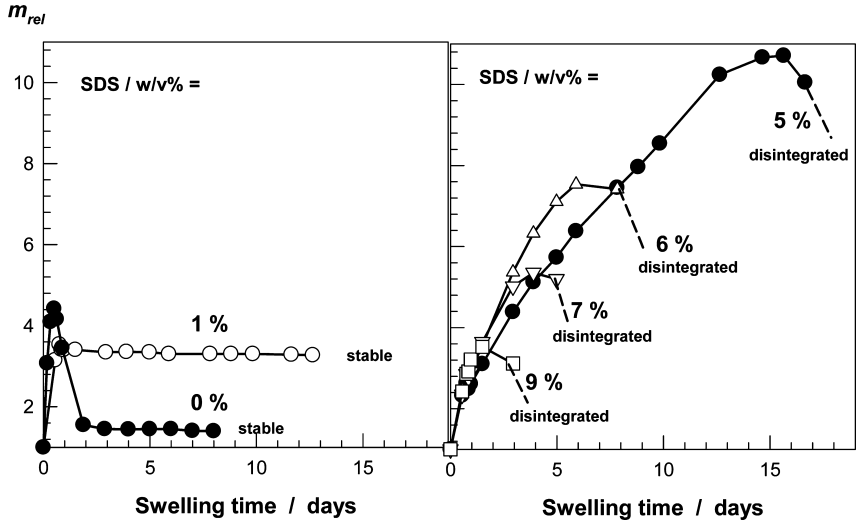

Figure 5. Relative weight swelling ratio m_{rel} of the gels formed at C_0 = 10% in aqueous SDS solutions shown as a function of the swelling time. SDS concentrations in the external solutions are indicated.

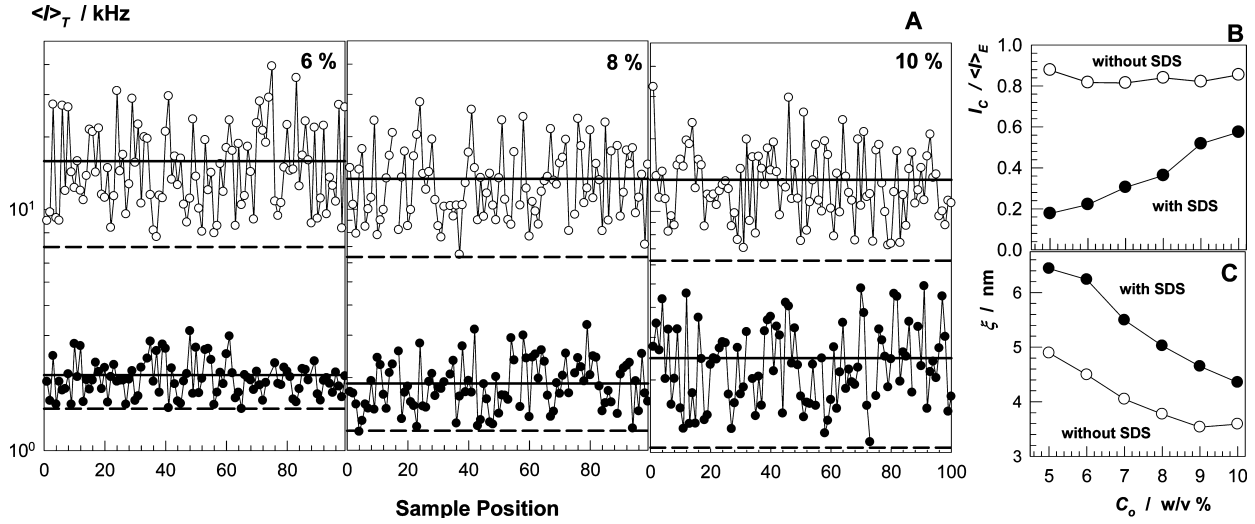

Figure 6. (A) Variation of $\langle I\rangle_T$ with the sample position of the physical gels with (●) and without SDS (○). The initial monomer concentrations C_0 are indicated. (B, C) Contribution of the static component $I_C/\langle I\rangle_E$ of the scattered intensity (B) and the dynamic correlation length ξ (C) plotted against C_0.

variations of $\langle I\rangle_T$ with randomly chosen sample position for gels with (filled symbols) and without SDS (open symbols). Note that $\langle I\rangle_T$ is averaged over a measurement time of 30 s. The solid lines represent the ensemble-averaged scattering intensity, $\langle I\rangle_E$, obtained by averaging $\langle I\rangle_T$ over all sample positions. The dashed lines represent that part of the scattering intensities $\langle I_F\rangle_T$ which is due to liquidlike concentration fluctuations. Almost 1 order of magnitude increase of the spatial fluctuations in $\langle I\rangle_T$ is observed after extraction of SDS micelles from the hydrogels. Since the relative swelling ratio $m_{rel,eq}$ of the physical gels without SDS is around 1.3, this increase cannot be attributed to the dilution of the network chains. However, the presence of SDS can markedly affect the scattering contrast. It is thus advisible to use a relative measure to capture the inhomogeneity. In Figure 6B, the relative contribution of the static component (frozen structure) of the scattered intensity, $I_C/\langle I\rangle_E$ is plotted against C_0. An appreciable portion of the thermal scattering from gels containing SDS is due to the presence of large SDS micelles; $I_C/\langle I\rangle_E$ monotonically increases from 20% to 60% with rising C_0 due to the suppression of the fluctuations by the polymer chains. In the absence of SDS, $I_C/\langle I\rangle_E$ of gels is independent of C_0 and equals to 83 ± 3%. Thus, the degree of the spatial gel inhomogeneity considerably increases after extraction of surfactant molecules. This increase is possibly related to the loss of reversibility of the cross-linkages and the resulting increase in the apparent cross-link density of gels at long experimental time scales (Table 1). We calculated the correlation length ξ of gels on the basis of their fast modes. In Figure 6C, ξ is plotted against C_0. ξ of surfactant containing gels is slightly decreasing from 6 to 4 nm, indicating decreasing mesh size with rising C_0, and it further decreases after extraction of SDS micelles.

Mechanical Properties of Gels. Inspection of the stress relaxation data in Figures 4C and 4D reveals that, at a given time scale, the modulus of gels containing SDS remains unchanged as the strain γ_0 is increased from 1% to 100%, while in the absence of SDS, it rapidly decreases with γ_0. In Figure 7A, the data are replotted as the variation of the relaxation modulus $G(t)$ of gels with increasing strain at fixed times. In the case of gels with SDS, the extent of the linear viscoelastic regime is

dx.doi.org/10.1021/ma202672y | *Macromolecules* 2012, 45, 1991–2000

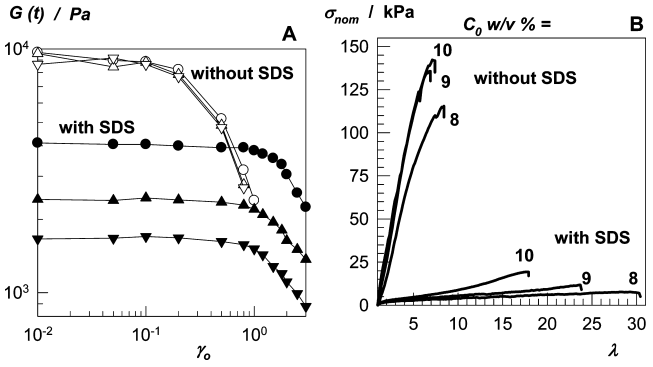

Figure 7. (A) Relaxation modulus $G(t)$ as a function of strain γ_0 for various times t for gels with (filled symbols) and without SDS (open symbols). t = 0.1 (circles), 1.0 (triangles up), and 10 s (triangles down). (B) Stress–strain curves of the physical gels with and without SDS formed at various C_0 indicated.

rather large, up to strains around 100%, whereas it is small and limited to strains up to ~10% for gels without SDS. This indicates a remarkable decrease of the toughness of gels after extraction of SDS micelles, as also observed by the uniaxial elongation tests conducted on cylindrical gel samples. Figure 7B represents tensile stress–strain data of the physical gels formed at three different concentrations C_0. In the presence of SDS, the elongation at break exceeds 1700%, and it further increases as C_0 is decreased. Without SDS, the gels break at about 700% strain and exhibit an order of magnitude larger ultimate strength as compared to the SDS containing gels.

The large strain properties of the physical gels with and without SDS were also compared by cyclic compression tests. The tests were conducted by compression of cylindrical gel samples at a constant crosshead speed to a predetermined maximum load, followed by immediate retraction to zero displacement. After a fixed waiting time of 2 min, the cycles were repeated several times. In all cases, the loading curve of the compressive cycle was different from the unloading curve, indicating damage in the gels and dissipation of energy during the cycle. In Figure 8A, three successive loading–unloading cycles of a gel sample formed at C_0 = 10% are shown as the dependence of the true stress σ_{true} on the deformation ratio λ. The behavior of virgin gel sample can be recovered when the sample is left to rest for 2 min without stress. The reversibility of loading/unloading cycles was observed in all gels with or without SDS. The perfect superposition of the successive loading curves demonstrates that the damage done to the gel samples during the loading cycle is recoverable in nature. This behavior is similar to that of the hydrogels formed by dynamic cross-links[32−34] but different from double-network gels showing irreversible fracture of the covalent bonds in the primary network.[35−37]

Figures 8B and 8C show the results of the loading/unloading experiments of the gels with increasing maximum load from 0.5 to 4 N. When SDS is present (B), a significant hysteresis is observed, while in the absence of SDS (C), the extent of hysteresis is low. In Figure 9A, the energy U_{hys} dissipated during the compression cycle calculated from the area between the loading and unloading curves is plotted against the maximum load. For gels without SDS, U_{hys} is below 3 kJ/m^3, while with SDS, it is much larger. The hysteresis increases with increasing maximum load, i.e., with increasing maximum strain during the loading step, or with decreasing monomer concentration C_0. The hysteresis energy U_{hys} of the present gels can be interpreted as the average dissociation energy U_{xl} of a hydrophobic association times the number of associations broken down during the compression cycle,[37,38] i.e.

$$U_{hys} = U_{xl}\nu_e f_\nu \tag{7}$$

where ν_e is the concentration of elastically effective hydrophobic associations, i.e., the cross-link density of physical gels, and f_ν is the fraction of associations broken during the loading/unloading cycle. We assume that the energy U_{xl} required for the detachment of the hydrophobe C18 from associations is of the order of 10^2 kJ/mol.[39,40] To estimate the cross-link density ν_e, the plateau moduli G_0 of gels are obtained from the constant value of G' at a high frequency (Figures 4A,B and Figure S6). Since G_0 corresponds to the shear modulus G, ν_e was calculated using the equation[41,42]

$$G = (1 - 2/\phi)\nu_e RT(\nu_2^0/\nu_2)^{2/3} \tag{8}$$

where ϕ is the functionality of the cross-links, R is gas constant, and T is the absolute temperature (K). The calculation using eq 8 assumes a phantom network behavior, which is generally appropriate for the transient networks. However, for the present gels formed by hydrophobic associations, since the average aggregation number is large,[43] the cross-link function-

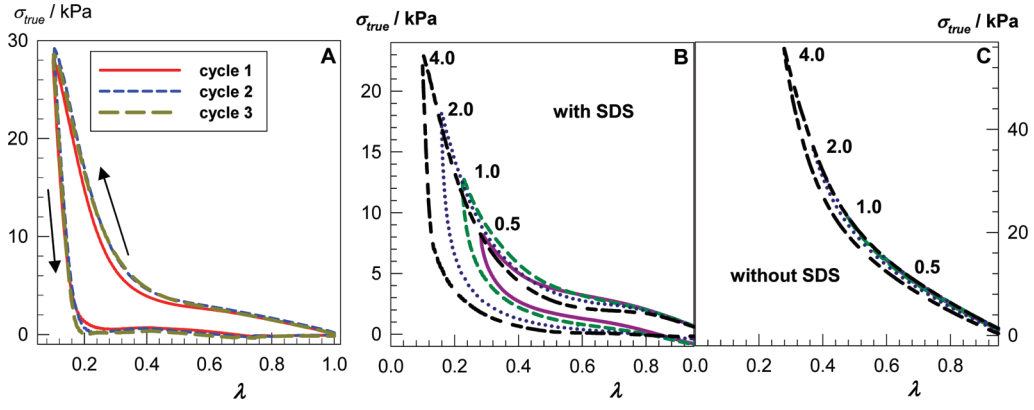

Figure 8. True stress σ_{true} vs deformation ratio λ curves from cyclic compression tests for the gel samples formed at C_0 = 10%. (A) Three successive loading/unloading cycles for a gel sample containing SDS. Maximum load = 5 N. (B, C) Loading/unloading cycles for gels with (B) and without SDS (C). The tests were conducted with increasing maximum load from 0.5 to 4 N, as indicated.

dx.doi.org/10.1021/ma202672y | Macromolecules 2012, 45, 1991–2000

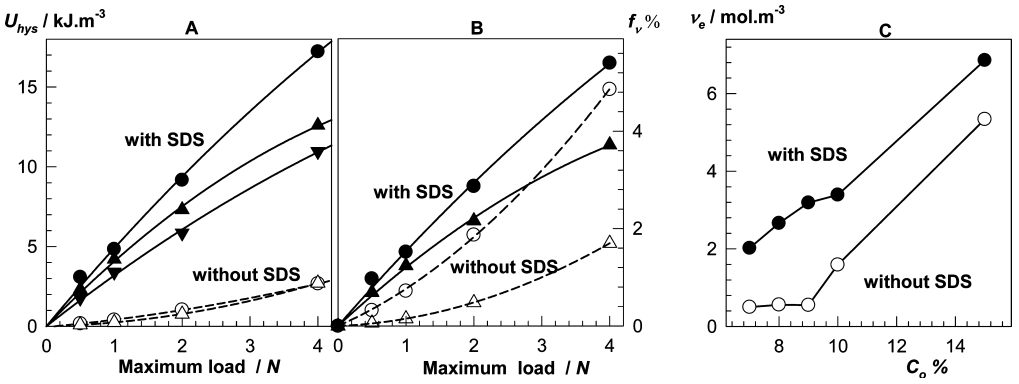

Figure 9. (A, B) Hysteresis energy U_{hys} (A) and the fraction f_ν of dissociated cross-links during the loading/unloading experiments (B) shown as a function of the maximum load. Data were from gels with (filled symbols) and without SDS (open symbols). C_0 = 9% (circles), 10% (triangles up), and 15% (triangles down). (C) Cross-link density ν_e of gels with (●) and without SDS (○) shown as a function of C_0.

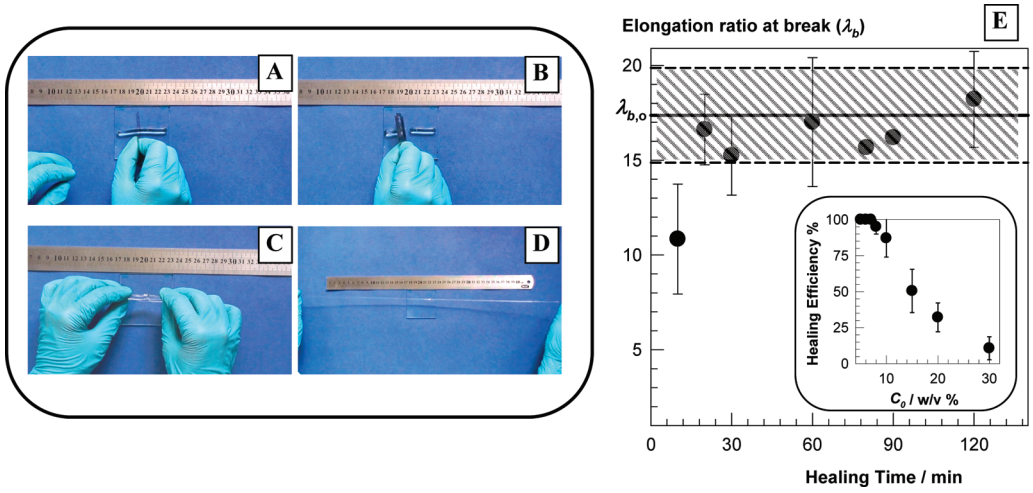

Figure 10. (A–D) Photographs of a gel sample formed at C_0 = 10%. After cutting into two pieces and pressing the fractured surfaces together for 10 min, they merge into a single piece. (E) Elongation ratio at break of healed gel samples (λ_b) formed at C_0 = 10% shown as a function of the healing time. The horizontal line and the dashed area represent the mean value and the standard deviation for the virgin gel sample. Inset to (E) shows the healing efficiency vs C_0 plot for a healing time of 30 min.

ality is also large, which will suppress the fluctuations of the cross-links about their mean positions,[44] so that the gels are expected to deform affinely, i.e., $(1 - 2/\phi) = 1$. Using the experimentally determined values of ν_2^0 and ν_2 (Table 1), together with the high-frequency elastic moduli G' (Figure S6), we calculated ν_e of gels with and without SDS and they are plotted in Figure 9C against C_0. Surfactant containing gels exhibit higher cross-link densities than the corresponding gels without SDS. This difference is possibly related to the effect of surfactant on the aggregation behavior of associating polymers in aqueous solutions. Since the presence of surfactant above its cmc weakens hydrophobic interactions, thereby reducing the aggregation number of hydrophobic blocks, the gels with SDS contain larger number of hydrophobic associations than without SDS, so that they exhibit higher cross-link densities. We have to mention that, at experimental time scales of the order of seconds, the apparent cross-link density of SDS containing gels is much lower than those without SDS due to the shorter lifetimes of the associations (cf. Figure 4).

Using the values of ν_e and U_{hys}, one may solve eq 7 for the fraction f_ν of physical cross-links reversibly broken during the compression cycles. The results are given in Figure 9B for the gels formed at C_0 = 9% and 10% plotted against the maximum load. When SDS is present (filled symbols), 1–6% of the physical cross-links dissociate under force, but reversibly, if the force is removed they re-form again. As C_0 is increased, f_ν decreases and becomes 0.3–2% at C_0 = 15%. In the absence of SDS (open symbols), this fraction is small at low maximum loads, indicating the stability of the associations, but it increases with increasing load and approaches to its value in SDS containing gels. The results thus reveal that there are a larger number of hydrophobic associations in physical gels with SDS, and these associations are easily broken; both of these properties contribute their significant hysteresis behavior in cyclic compression tests.

Reversible disengagements of the hydrophobic units from the associations under an external force point out the self-healing properties of surfactant containing physical gels. The Supporting Information movie shows the healing process of a gel sample formed at C_0 = 10%. The images in Figures 10A–D illustrate that when the fracture surfaces of a ruptured gel sample are pressed together at 24 °C, the two pieces merge into a single piece. The joint re-formed withstands very large extension ratios as the original gel sample before its fracture. No such self-healing behavior was observed after SDS had been extracted from the gel networks.

To quantify the healing efficiency, tensile testing experiments were performed using cylindrical gel samples of 5 mm diameter

dx.doi.org/10.1021/ma202672y | *Macromolecules* 2012, 45, 1991–2000

and 6 cm length. The samples were cut in the middle, and then the two halves were merged together within a plastic syringe (of the same diameter as the gel sample) at 24 °C by slightly pressing the piston plunger. The healing time was varied from 10 to 130 min, and each experiment was carried out starting from a virgin sample. In Figure 10E, the elongation ratio at break of the healed gel sample (λ_b) formed at C_0 = 10% is plotted against the healing time. The horizontal solid line represents the average elongation ratio at break of the virgin sample ($\lambda_{b,0}$) with a standard deviation indicated by the dashed area (17.4 ± 2.5%). Healing efficiency, $\lambda_b/\lambda_{b,0}$, rapidly increases with the healing time, and after 20 min, a healing efficiency of nearly 100% was observed. We note that, although the stress−strain curves of the healed gels superimposed for all healing times, gel samples healed longer than 1 h broke at a different location than the healed zone. Experiments were also conducted using the gels formed at various C_0. In this set of experiments, the healing efficiency was determined for a fixed healing time of 30 min. As illustrated in the inset to Figure 10E, the healing efficiency remarkable decreases with C_0, i.e., with decreasing fraction of dissociable cross-links (Figure 9B); as a consequence, the damage created in the gel samples remained permanent at high polymer concentrations.

All the above dynamic and mechanical features of the physical gels suggest that the key factor leading to the self-healing behavior is the weakening of strong hydrophobic interactions due to the presence of surfactant molecules. Before fracture, this weakening creates an energy dissipation mechanism along the gel samples so that the degree of toughness significantly increases. After fracture, hydrophobes can easily find their partners in the other cut surface due to the hydrophobic interactions across the damage surfaces together with the help of the internal dynamics so that self-healing of the damaged gel samples occurs within a short period of time.

CONCLUSIONS

As a main finding of our experiments, several dynamic characteristics of self-healing hydrogels formed via micellar polymerization technique vanish after extraction of surfactant micelles. Physical gels containing SDS exhibit, in addition to the fast mode, a slow relaxation mode in DLS, indicating structural relaxations on the time scales of milliseconds. Time-dependent dynamic moduli of these gels also indicate the temporary nature of the hydrophobic associations having lifetimes of the order of seconds to milliseconds. After extraction of SDS, however, the gels behave similar to chemically cross-linked gels with time-independent dynamic moduli and a single relaxation mode in DLS. The results thus show that, when SDS micelles are present, the cross-links are reversible due to the local solubilization of the hydrophobic associations, while after extraction of SDS, direct exposure of the hydrophobic associations to the aqueous environment considerably increases their lifetimes. This structural change in the physical gels due to the removal of SDS is responsible for their insolubility in water and solubility in SDS solutions. A significant increase in the degree of spatial gel inhomogeneity was observed after extraction of surfactant molecules, which is also related to the breakdown of the reversible nature of the cross-linkages and resulting increase in the apparent cross-link density of gels at long time scales. In the presence of SDS, the gels are very tough and the elongation at break exceeds 1700% while without SDS, the gels break at about 700% strain and exhibit an order of magnitude larger ultimate strength. Results of the cyclic compression tests show that a large number of physical cross-links in SDS containing gels dissociate under force, but reversibly, if the force is removed, they re-form again. The reversible disengagements of the hydrophobic units building the physical cross-links leads to a healing efficiency of nearly 100%, while no such self-healing behavior was observed after extraction of SDS from the gel networks. The loss of self-healing ability of the present gels after their swelling limits their application areas to systems in which the gel samples have to be isolated from the environment.

ASSOCIATED CONTENT

Supporting Information

Figure S1, solubility of C18 in aqueous SDS−NaCl solutions; Figure S2, G' vs reaction time profiles of the micellar copolymerization of AAm and C18 and the limiting values of G' and tan δ as a function of C_0; Figure S3, the decomposition plots according to eq 3; Figure S4, the relaxation rate distribution functions $G(\Gamma)$ of surfactant solutions and gels; Figure S5, the stress−strain curves of the hydrogels; and Figure S6, the results of the frequency sweep tests conducted on the hydrogels with and without SDS. This material is available free of charge via the Internet at http://pubs.acs.org.

AUTHOR INFORMATION

Notes

The authors declare no competing financial interest.

ACKNOWLEDGMENTS

Work was supported by the Scientific and Technical Research Council of Turkey (TUBITAK) and International Bureau of the Federal Ministry of Education and Research of Germany (BMBF), TBAG-109T646. O.O. thanks the Turkish Academy of Sciences (TUBA) for the partial support.

REFERENCES

(1) Candau, F.; Selb, J. *Adv. Colloid Interface Sci.* **1999**, *79*, 149.
(2) Volpert, E.; Selb, J.; Candau, F. *Polymer* **1998**, *39*, 1025.
(3) Hill, A.; Candau, F.; Selb, J. *Macromolecules* **1993**, *26*, 4521.
(4) Regalado, E. J.; Selb, J.; Candau, F. *Macromolecules* **1999**, *32*, 8580.
(5) Candau, F.; Regalado, E. J.; Selb, J. *Macromolecules* **1998**, *31*, 5550.
(6) Kujawa, P.; Audibert-Hayet, A.; Selb, J.; Candau, F. *J. Polym. Sci., Part B: Polym. Phys.* **2004**, *42*, 1640.
(7) Kujawa, P.; Audibert-Hayet, A.; Selb, J.; Candau, F. *Macromolecules* **2006**, *39*, 384.
(8) Gao, B.; Guo, H.; Wang, J.; Zhang, Y. *Macromolecules* **2008**, *41*, 2890.
(9) Tuncaboylu, D. C.; Sari, M.; Oppermann, W.; Okay, O. *Macromolecules* **2011**, *44*, 4997.
(10) Chern, C. S.; Chen, T. J. *Colloids Surf., A* **1998**, *138*, 65.
(11) Leyrer, R. J.; Machtle, W. *Macromol. Chem. Phys.* **2000**, *201*, 1235.
(12) Lau, W. *Macromol. Symp.* **2002**, *182*, 283.
(13) Rehage, H.; Hoffman, H. *Mol. Phys.* **1991**, *74*, 933.
(14) (a) Missel, P. J.; Mazer, N. A.; Benedek, G. B.; Young, C. Y. *J. Phys. Chem.* **1980**, *84*, 1044. (b) Magid, L. J. *J. Phys. Chem. B* **1998**, *102*, 4064. (c) Hassan, P. A.; Raghauan, S. R.; Kaler, E. W. *Langmuir* **2002**, *18*, 2543. (d) Sutherland, E.; Mercer, S. M.; Everist, M.; Leaist, D. *J. Chem. Eng. Data* **2009**, *54*, 272.
(15) Joosten, J. G. H.; Mccarthy, J. L.; Pusey, P. N. *Macromolecules* **1991**, *24*, 6690.
(16) Pusey, P. N.; van Megen, W. *Physica A* **1989**, *157*, 705.
(17) Ikkai, F.; Shibayama, M. *Phys. Rev. Lett.* **1999**, *82*, 4946.

(18) ISO 7875-1, 1996. Water quality. Determination of surfactants. Part 1: Determination of anionic surfactants by measurement of the methylene blue index (MBAS). USO/TC 147.
(19) Kizilay, M. Y.; Okay, O. *Polymer* **2003**, *44*, 5239.
(20) Gundogan, N.; Melekaslan, D.; Okay, O. *Macromolecules* **2002**, *35*, 5616.
(21) The network chains are in the Gaussian regime up to a linear swelling ratio α around 1.5 (cf. ref 20). In this regime, the elastic modulus decreases with increasing degree of swelling.
(22) Förster, S.; Schmidt, M.; Antonietti, M. *Polymer* **1990**, *31*, 781.
(23) Young, C. Y.; Missel, P. J.; Mazer, N. A.; Benedek, G. B.; Carey, M. C. *J. Phys. Chem.* **1978**, *82*, 1375.
(24) Hayashi, S.; Ikeda, S. *J. Phys. Chem.* **1980**, *84*, 744.
(25) Magid, L. J.; Li, Z.; Butler, P. D. *Langmuir* **2000**, *16*, 10028.
(26) Molchanov, V. S.; Philippova, O. E.; Khokhlov, A. R.; Kovalev, Y. A.; Kuklin, A. I. *Langmuir* **2007**, *23*, 105.
(27) Kumar, S.; Bansal, D.; Din, K. *Langmuir* **1999**, *15*, 4960.
(28) Kunieda, H.; Ozawa, K.; Huang, K.-L. *J. Phys. Chem. B* **1998**, *102*, 831.
(29) Siriwatwechakul, W.; LaFleur, T.; Prud'homme, R. K.; Sullivan, P. *Langmuir* **2004**, *20*, 8970.
(30) Sato, T.; Acharya, D. P.; Kaneko, M.; Aramaki, K.; Singh, Y.; Ishitobi, M.; Kunieda, H. J. *J. Dispersion Sci. Technol.* **2006**, *27*, 611.
(31) Patist, A.; Oh, S. G.; Leung, R.; Shah, D. O. *Colloids Surf., A* **2001**, *176*, 3.
(32) Miquelard-Garnier, G.; Creton, C.; Hourdet, D. *Soft Matter* **2008**, *4*, 1011.
(33) Miquelard-Garnier, G.; Hourdet, D.; Creton, C. *Polymer* **2009**, *50*, 481.
(34) Lin, W. C.; Fan, W.; Marcellan, A.; Hourdet, D.; Creton, C. *Macromolecules* **2010**, *43*, 2554.
(35) Tanaka, Y.; Fukao, K.; Miyamoto, Y. *Eur. Phys. J. E* **2000**, *3*, 395.
(36) Tanaka, Y.; Kuwabara, R.; Na, Y. H.; Kurokawa, T.; Gong, J. P.; Osada, Y. *J. Phys. Chem. B* **2005**, *109*, 11559.
(37) Webber, R. E.; Creton, C.; Brown, H. R.; Gong, J. P. *Macromolecules* **2007**, *40*, 2919.
(38) Lake, G. J.; Thomas, A. G. *Proc. R. Soc. London, A* **1967**, *300*, 108.
(39) Annable, T.; Buscall, R.; Ettelaie, R.; Whittlestone, D. *J. Rheol.* **1993**, *37*, 695.
(40) Ng, W. K.; Tam, K. C.; Jenkins, R. D. *J. Rheol.* **2000**, *44*, 137.
(41) Flory, P. J. *Principles of Polymer Chemistry*; Cornell University Press: Ithaca, NY, 1953.
(42) Treloar, L. R. G. *The Physics of Rubber Elasticity*; Oxford University Press: Oxford, UK, 1975.
(43) Shashkina, Yu. A.; Zaroslov, Yu. D.; Smirnov, V. A.; Philippova, O. E.; Khokhlov, A. R.; Pryakhina, T. A.; Churochkina, N. A. *Polymer* **2003**, *44*, 2289.
(44) Mark, J. E.; Erman, B. *Rubberlike Elasticity. A Molecular Primer*; Cambridge University Press: Cambridge, UK, 2007.